

Interpreting ecological patterns generated through simple stochastic processes

Kirk A. Moloney^{1, 2, 3}, Antoine Morin^{1, 3, 4}, and Simon A. Levin^{1, 2, 3}

¹Section of Ecology and Systematics, Corson Hall, Cornell University, Ithaca, NY 14853-2701 USA;

²Ecosystems Research Center, Corson Hall, Cornell University, Ithaca, NY 14853-2701 USA; ³Center for Environmental Research, Hollister Hall, Cornell University, Ithaca, NY 14853 USA; and

⁴Department of Biology, University of Ottawa, Ottawa, Ontario K1N 6N5, Canada

Abstract

The analysis of spatial patterns is fundamental to understanding ecological processes across geographic scales. Through an analysis of two simple, one-dimensional stochastic models, we develop a framework for identifying the scale of processes producing pattern. We show that for some simple model systems spectral analysis identifies exactly the scale of pattern formation. In other, more complicated systems, autocorrelation analysis appears to yield greater insight into the scale of the dynamics producing pattern; in these, the relative importance of processes at different scales can be determined directly from the change in slope of the autocorrelation function.

In general, it is not possible to state which technique will be most useful in the analysis of pattern. Spectral analysis and autocorrelation analysis represent duals that can be extended and applied to more complex systems, potentially yielding insight into the nature of a wide variety of spatially determined ecological processes.

Introduction

Interest in the issue of ecological scale has grown dramatically in recent years, in part because of the increasing availability of large scale images obtained through remote sensing and in part because of a growing concern regarding large scale environmental problems (e.g., Gardner *et al.* 1987; Krummel *et al.* 1987; Milne 1988; Levin 1989; Powell 1989; Wiens 1989).

It has long been recognized that the composition of ecological communities varies over large spatial scales in response to broad changes in soil structure, topography, climate, etc. (Whittaker 1975). The dynamics structuring communities also can vary over very small spatial scales (e.g., Moloney 1988, 1990). Indeed, patterning and patchiness can be recognized at virtually every scale of investigation

(Haury *et al.* 1977; Krummel *et al.* 1987). Until recently, few analytical techniques have been available to allow the study of the relationship between pattern, scale, and ecosystem dynamics. However, a growing number of authors have been exploring the utility of methods such as percolation theory (Gardner *et al.* 1987; Turner *et al.* 1989), fractal geometry (Krummel *et al.* 1987; Gardner *et al.* 1987; Milne 1988), semivariance analysis (Robertson 1987; Robertson *et al.* 1988), autocorrelation analysis (Ord 1979), cross-correlation analysis (Weber *et al.* 1986), and spectral analysis (Platt and Dennman 1975; Ord 1979) in identifying the relationship between ecological pattern and process. The present paper develops a preliminary framework for employing spectral analysis and autocorrelation analysis in the determination of the processes producing pattern in ecological systems.

Typically, ecologists have employed spectral analysis and autocorrelation analysis to find hidden periodicities in the distribution of organisms in space, or to model population processes that have a cyclic component. However, these methods have also been used to good advantage by oceanographers and geologists in the study of patterns of spatial variability in systems for which the underlying dynamic is not periodic. An essential step in the application of these techniques is to develop a catalogue of the patterns produced by fairly simple processes. In this paper, we examine two classes of stochastic model that generate spatial patterns, and examine the form of those patterns as portrayed by spectral analysis and autocorrelation analysis. The study of pattern formation in simple models is a first step in the interpretation of patterns in nature (Levin and Segel 1985). However, since quite different models can give rise to similar patterns, the creation of a catalogue of patterns is only a first step in this process.

The first model examined in this paper is based on a simple moving average (MA) process and can be used to characterize pattern formation in systems where individual organisms occur in localized clusters or patches, e.g., clonal plants or plants with very short dispersal distances, swarms of insects, or schools of fish. In the MA model, aggregations of organisms occur in discrete patches; when patches overlap, local density is determined as the sum of the densities of the overlapping patches, i.e., the process of patch formation is additive.

The second model considers patch forming processes that are non-additive. This is appropriate when interest centers on a character such as disturbance. In this case the local state of the system is determined only by whether or not the site is within a patch, and there is no additional effect introduced through the overlap of multiple patches. There are many examples of this type of process in the ecological literature, most of which derive from systems structured by disturbances; wherever a disturbance occurs the system is reset to an early successional value that is substantially different in structure from the surrounding undisturbed sites (e.g., see Levin and Paine (1974) and Paine and Levin (1981) for an example in marine ecosystems; Hobbs and

Mooney (1985) for serpentine grassland; Reiners and Lang (1979) for forested ecosystems).

We derive expressions for the autocorrelation function and power spectrum corresponding to the two stochastic models investigated and use these functions to characterize spatial pattern. Initial development is in terms of monotypic patch distributions; in later sections we extend our approach to analyze the effect of including a mixture of patches of different size-scales in each model.

Patch formation as a moving average process

The first patch forming process we consider can be modeled as a moving average (MA) process. The MA model describes the formation of aggregations of organisms in one dimension, according to a very simple rule: patches of organisms are deposited independently and at random. To simplify our analysis initially, we will assume that all patches are identical in size, which in a one dimensional system means that they all have the same width.

It is not wholly unrealistic to consider a one dimensional system in modeling pattern formation, as ecological studies of pattern are often confined to one dimension. For example, a commonly employed sampling design in plant ecology is to determine plant densities in contiguous quadrats along a transect (e.g., Greig-Smith 1952; Ripley 1978; Dale and MacIsaac 1989). Each quadrat then represents a discrete sampling unit in a one dimensional series. A similar one dimensional design has also been used in oceanographic studies of krill and phytoplankton distributions (Weber *et al.* 1986; Levin *et al.* 1989b).

In modeling a patch forming process as an MA process, a certain perspective must be adopted: Although there are necessarily two edges to a patch, we will consider the first edge of a patch encountered along a one dimensional transect to be the point of patch initiation (left edges in Fig. 1). Patches, since they are all of the same size, have a width of $m + 1$ sampling units. The probability that patch initiation occurs at any point s along a transect can then be represented by a binomially distributed random variable, Z_s , that evaluates to

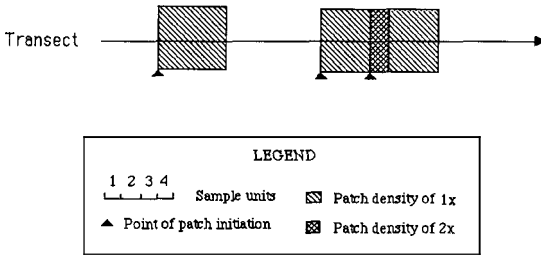


Fig. 1. Characterization of a one-dimensional MA process involving randomly placed patches of uniform width.

1, if patch initiation occurs, or to 0, if patch initiation does not occur. The impact of patch initiation at position s on a position i units to the patch side of s (to the right in Fig. 1) is to change local density by a factor of β_i ($\beta_i = 0$ for $i < 0$ and $i > m$). This is a direct result of position $s + i$ ($i = 0, m$) lying within the patch. Given these definitions, we can model the patch forming process as:

$$X_s = \beta_0 Z_s + \beta_1 Z_{s-1} + \dots + \beta_m Z_{s-m}, \quad (1)$$

where X_s is density at point s . Since patch width is constant at $m + 1$ units, X_s represents the additive effect of patch initiation events occurring within an $m + 1$ unit wide region of the transect. (An implicit assumption in Eq. 1 is that the density is 0 for positions not affected by a patch, although this can be easily changed through a modification of the formula).

In order to calculate the power spectrum of the patch forming process described by Eq. 1, we center the system so that X_s has a mean value of zero. Once this is done, let k represent the lag (or distance) between points in the system. The autocorrelation function, $\rho(k)$, of the patch forming process is then given by

$$\rho(k) = \left(\sum_{i=0}^{m-k} \beta_i \beta_{i+k} \right) / \left(\prod_{i=0}^m \beta_i^2 \right), \quad (2)$$

yielding the discrete power spectrum $f(\omega)$,

$$f(\omega) = (1/\pi) \cdot \left[1 + 2 \prod_{k=1}^m \rho(k) \cdot \cos(\omega k) \right], \quad (3)$$

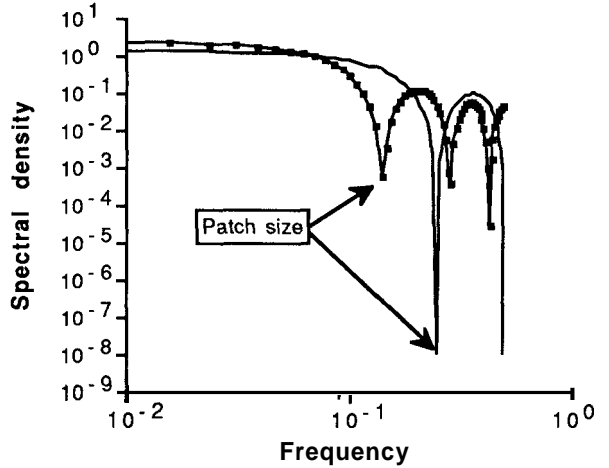


Fig. 2. Power spectra for two MA patch-forming processes. The plain line represents the spectrum for a process with a patch width of 4 measurement units and the line connecting solid squares represents the spectrum for a process with a patch width of 7 units.

where w is frequency in radians (Chatfield 1984).

In the special case where patches are of uniform density, we can set all the β_i equal to 1 by rescaling X_s , leading to simplified expressions for the autocorrelation function

$$\rho(k) = [m + 1 - k] / [m + 1]. \quad (2')$$

and the power spectrum (when Eq. 2' is substituted into Eq. 3).

The pattern portrayed by the power spectrum associated with Eq. 2' has an interesting relationship to the underlying patch forming process. Since $f(0) > 0$, $f'(0) = 0$ (see Eq. 4 below) and $f''(0) < 0$, the first positive minimum of $f(w)$ is the first positive zero of the derivative:

$$f'(\omega) = (-2/(\pi(m+1))) \cdot \prod_{k=1}^m [k(m-k+1) \cdot \sin(\omega k)] = 0. \quad (4)$$

This occurs at $\omega = 2\pi/(m+1)$, corresponding to a wavelength of $m + 1$ units, the patch size (see the Appendix for a proof of this statement). Therefore, the characteristic patch size producing pattern in the system can be recovered as the first minimum of $f(\omega)$ on the positive side of the origin, i.e., $\omega > 0$ (Fig. 2).

Thus, for an MA process of uniform density in one dimension, the power spectrum can be used to identify exactly the scale of the process that is producing pattern. This represents a very powerful technique for linking the scale of a process to the pattern produced, particularly as the spectrum is very easy to calculate directly from raw data (see Chatfield 1984; Press *et al.* 1986). It should be pointed out that this technique works because the process is one dimensional, and does not extend cleanly to two dimensions, or to systems where the patches are not of uniform density. We will return to these problems in a later section.

Patch formation as a non-additive process

The second patch forming process we consider is patterned after phenomena that are non-additive in their impact upon ecological systems. For example, in many situations a site affected by multiple overlapping disturbances is indistinguishable from a site affected by only one disturbance. Like the MA model, the model for non-additive processes describes the distribution of patches (e.g., disturbances) in one-dimension, according to a very simple rule: patches are distributed independently and at random. As in the first model, all patches are of the same width, $m + 1$ units; but unlike the MA model the system has only two states: patch and non-patch, with densities Q and P , respectively. Again, the left edge of a patch is considered to be the point of patch initiation.

The first step in studying the pattern forming properties of the non-additive process is to derive the autocorrelation function. The probability that a patch is initiated at any one point will be denoted as q , with $p = 1 - q$ representing the probability that a patch is not initiated. If the state of the system at point s is represented as X_s , then the expected value of X_s is given by

$$E[X_s] = P \cdot p^{m+1} + Q(1 - p^{m+1}). \quad (5)$$

The system can be centered by taking new values for P and Q ,

$$P' = P - E[X_s] = [P - Q][1 - p^{m+1}] \quad (6)$$

$$Q' = Q - E[X_s] = [Q - P]p^{m+1}. \quad (7)$$

The probabilities that two points separated by a lag $k \leq (m + 1)$ are both located in at least one patch ($F_{QQ}(k)$), that one point is located in a patch and the other is not ($F_{QP}(k)$), and that both points lie outside of patches ($F_{PP}(k)$) are determined as follows:

$$F_{QQ}(k) = [1 - p^{m+1-k}] + [1 - p^k]^2 p^{m+1-k} \quad (8)$$

$$F_{QP}(k) = 2 \cdot [p^{m+1-k}][1 - p^k] p^k \quad (9)$$

$$F_{PP}(k) = [p^{m+1-k}] p^{2k}. \quad (10)$$

In Eq. 8, the first term on the right of the equality is the probability that two points separated by a lag of k are located in the same patch; the second term is the probability that two points separated by a lag of k are located in two different patches. Similar equations apply for the case $k > m + 1$, but with k replaced by $m + 1$.

Given the previous definitions, the autocovariance function, $\gamma(k)$, for the non-additive process can be written as

$$\gamma(k) = Q'^2 F_{QQ}(k) + P'Q' F_{QP}(k) + P'^2 F_{PP}(k), \quad (11)$$

or more simply

$$\gamma(k) = (P' - Q')^2 [p^{m+1+\min(k, m+1)} - p^{2m+2}]. \quad (11')$$

This yields the autocorrelation function

$$\rho(k) = \frac{\gamma(k)}{\gamma(0)} = \frac{p^{\min(k, m+1)} - p^{m+1}}{1 - p^{m+1}}. \quad (12)$$

The autocorrelation function for the non-additive process depends on two parameters: patch size ($m + 1$) and the probability of patch initiation (q). In contrast, the autocorrelation function for

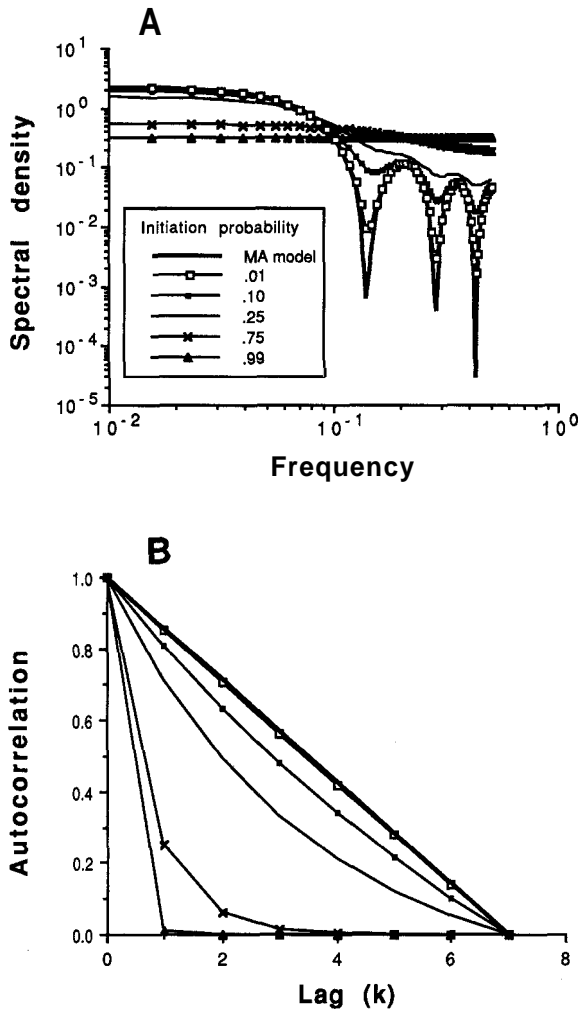


Fig. 3. Power spectra and autocorrelation relationships for an MA process and for a non-additive patch-forming process at 5 patch initiation levels, as described in the text. Patches were 7 units wide in all of the processes represented by the figure. A) Power spectra. B) Autocorrelation relationships.

the MA process is completely defined by one parameter, patch size. It is also of interest to note that the autocorrelation functions for the two processes are approximately equal when the probability of patch initiation is low ($q = 0$), since by L'Hôpital's Rule

$$\lim_{p \rightarrow 1} \rho(k) = (m+1-k)/(m+1). \quad (13)$$

Thus for the non-additive process, in the limit as

$p \rightarrow 1$, a minimum in the power spectrum is recovered at a frequency corresponding to the patch size, as in the MA process; for example, a patch size of 7 can be recognized as the first minimum in the spectrum of the non-additive process for values of $q \leq 0.10$ (Fig. 3a). Thus, values for q that allow detection of patch size from the power spectrum represent low to moderate levels of patch formation. However, if patch formation is a relatively common occurrence ($q \gg 0.10$), the autocorrelation function for the non-additive process drops off to zero much more rapidly than in the MA process (Fig. 3b) and the spectrum flattens (Fig. 3a). A flat spectrum is characteristic of a system dominated by pure white noise and, in the non-additive process, represents the case where patch formation is widespread, areas not affected by patch formation are randomly arrayed in space, and areas of patch (and non-patch) tend to be random in size due to the high probability of patch overlap.

Mixed patch models

The derivation of models for the MA process and non-additive process presented previously only considered patches of uniform size. This assumption is not directly applicable to ecological systems where patch widths measured by a one-dimensional transect will vary in size, even if patches are completely uniform and radially symmetrical. For example, in a system characterized by circular disturbances the patch widths measured by a one dimensional transect will vary in length from the diameter of the patch at one extreme to a point at the other. In this section we will extend the models to consider ecological systems composed of a mixture of patch-types.

Moving average process

The notation used to develop the mixed patch-type extension of the MA model will be the same as in the initial derivation, with a few modifications. Let n equal the number of patch types sampled by a

transect, with the width characterizing each patch-type i being equal to $m_i + 1$. The density (Q) within a patch is assumed to be uniform and is the same regardless of patch type. Also, local density produced by overlapping patches is assumed to be additive. A further assumption is that the patch types are distributed at random and independently of one another.

An MA model characterizing the system can be written as follows:

$$X_s = \prod_{i=1}^n \prod_{j=0}^{m_i} \beta_{ij} Z_{i(s-j)}. \quad (14)$$

Z_{is} represents the state of a binomially distributed random variable at point s that is associated with the initiation of patches of type i and takes on values of 1 or 0 with a probability of ζ_i and $1 - \zeta_i$, respectively. A patch of type i is initiated at any point s where $Z_{is} = 1$. Furthermore, the variance of Z_{is} will be given by σ_i^2 . As in the original analysis we will set all the β_{ij} terms in Eq. 14 equal to 1. Since the distribution of patch types is independent, the variance of X , is given by

$$\text{Var}(X_s) = \prod_{i=1}^n \sigma_i^2 [m_i + 1]. \quad (15)$$

From the above considerations it follows directly that the generalized autocorrelation function at lag k for the mixed patch-type MA model is given by

$$\rho(k) = \frac{\sum_{i=1}^n \sigma_i^2 [m_i + 1 - \min(k, m_i + 1)]}{\prod_{i=1}^n \sigma_i^2 [m_i + 1]} \quad (16)$$

This function and the corresponding function for the power spectrum require patch size and variance of patch initiation for each patch type as parameters, whereas only patch size was necessary to parameterize the simpler one patch-type model. As a consequence, the simple relationship found in the original analysis, a minimum in the power spectrum at a frequency corresponding to the patch width, does not necessarily present itself in the mixed patch-type model.

We have analyzed a mixed patch-type MA process using a simulation that places patches of more than one size at random along a one dimensional transect. Positions along the transect not affected by a patch were given a value of zero; positions affected by one patch were given a value of one; positions affected by two patches were given a value of two; etc. After each model run, the resulting data transects were centered before analysis. In the simplest case, two patch types – one three units wide and the other five units wide – were entered into simulations at varying frequencies to determine the effect on the resulting autocorrelation function and spectrum (Fig. 4). The two extreme cases, which involved only one of the two patch types in the patch forming process, were used as a reference. The power spectra for the mixed patch processes were all intermediate between the spectra of the two extreme cases (Fig. 4a). The particular shape of the spectral curve depends upon the relative frequency of the two patch types in the system. If the system is dominated by a patch type of size 5 then the power spectrum shows a first minimum corresponding closely to the first minimum for a pure patch type 5 process (Fig. 4a). For a system dominated by a patch type of size 3 it is more difficult to determine the patch type dominating the system. In the latter case, the first harmonic for patch type 5 – located at a frequency of 0.4 – dominates the system and draws the first minimum in the power spectrum towards a higher frequency (Fig. 4a). This leads to an underestimation of the width of the patch-type dominating the system.

The underlying structure of the mixed patch-type model is perhaps easier to interpret through the autocorrelation function (Fig. 4b). The size of patch types can be identified, since the slope of the autocorrelation function changes only at lags corresponding to the width of patch types producing pattern; the slope, which is negative, becomes less negative as the autocorrelation relationship attributable to each patch type cuts off. Furthermore, it is possible to determine the proportion of the variance in the system attributable to initiation events for each patch type by analyzing the change in slope of the autocorrelation function:

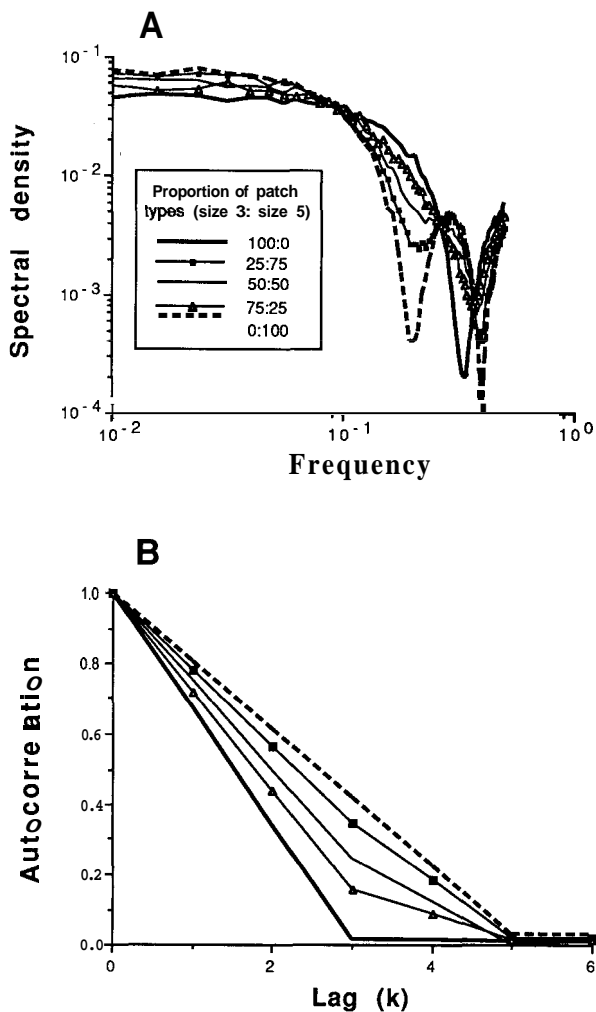


Fig. 4. Autocorrelation relationships and power spectra for a mixed patch-type MA process with varying proportions of size 3 and size 5 patches, as determined through analysis of a simple one-dimensional simulation model (see text regarding methods used in running the simulation). A) Power spectra. B) Autocorrelation relationships.

$$\sigma_i^2 = \text{Var}(X_s)[\rho(m_i+2) + \rho(m_i) - 2\rho(m_i+1)], \quad (17)$$

with total variance attributable to a patch of type i being equal to $\sigma_i^2(m_i+1)$. Thus, the autocorrelation function for a mixed patch-type MA process provides direct information regarding both the size of patches occurring within the system and the variance attributable to each patch type. In fact, the distribution of patch sizes can be determined exact-

ly through additional analysis of the variance relationship in Eq. 17, but only if patch initiation is a binomial process, patch formation is additive, and patches are of uniform density. These restrictions are rarely met in ecological systems. However, as shown below, useful information regarding the distribution of patch sizes in more complex systems can still be obtained from the autocorrelation relationship.

Non-additive processes

As in the MA model, a few minor changes in notation are necessary to modify the model for the non-additive process to allow a mixture of patch types. Let q_i represent the probability that a patch of type i is initiated at a point and let p_i represent the probability that it is not initiated. As in the MA model, the width characterizing a particular patch type is defined to be $m_i + 1$. It can then be easily shown that Equations 8 through 10 become

$$F_{QQ}(k) = [1 - \prod_{i=1}^n p_i^{m_i+1 - \min(k, m_i+1)}] + \quad (18)$$

$$[1 - \prod_{i=1}^n p_i^{\min(k, m_i+1)}]^2 \prod_{i=1}^n p_i^{m_i+1 - \min(k, m_i+1)}$$

$$F_{QP}(k) = 2 \cdot [\prod_{i=1}^n p_i^{m_i+1 - \min(k, m_i+1)}]$$

$$[1 - \prod_{i=1}^n p_i^{\min(k, m_i+1)}] \prod_{i=1}^n p_i^{\min(k, m_i+1)} \quad (19)$$

$$F_{PP}(k) = [\prod_{i=1}^n p_i^{m_i+1 - \min(k, m_i+1)}] \prod_{i=1}^n p_i^{2\min(k, m_i+1)}, \quad (20)$$

which yields the autocorrelation function

$$\rho(k) = \frac{\gamma(k)}{\gamma(0)} = \frac{\prod_{i=1}^n p_i^{\min(k, m_i+1)} - \prod_{i=1}^n p_i^{m_i+1}}{1 - \prod_{i=1}^n p_i^{m_i+1}} \quad (21)$$

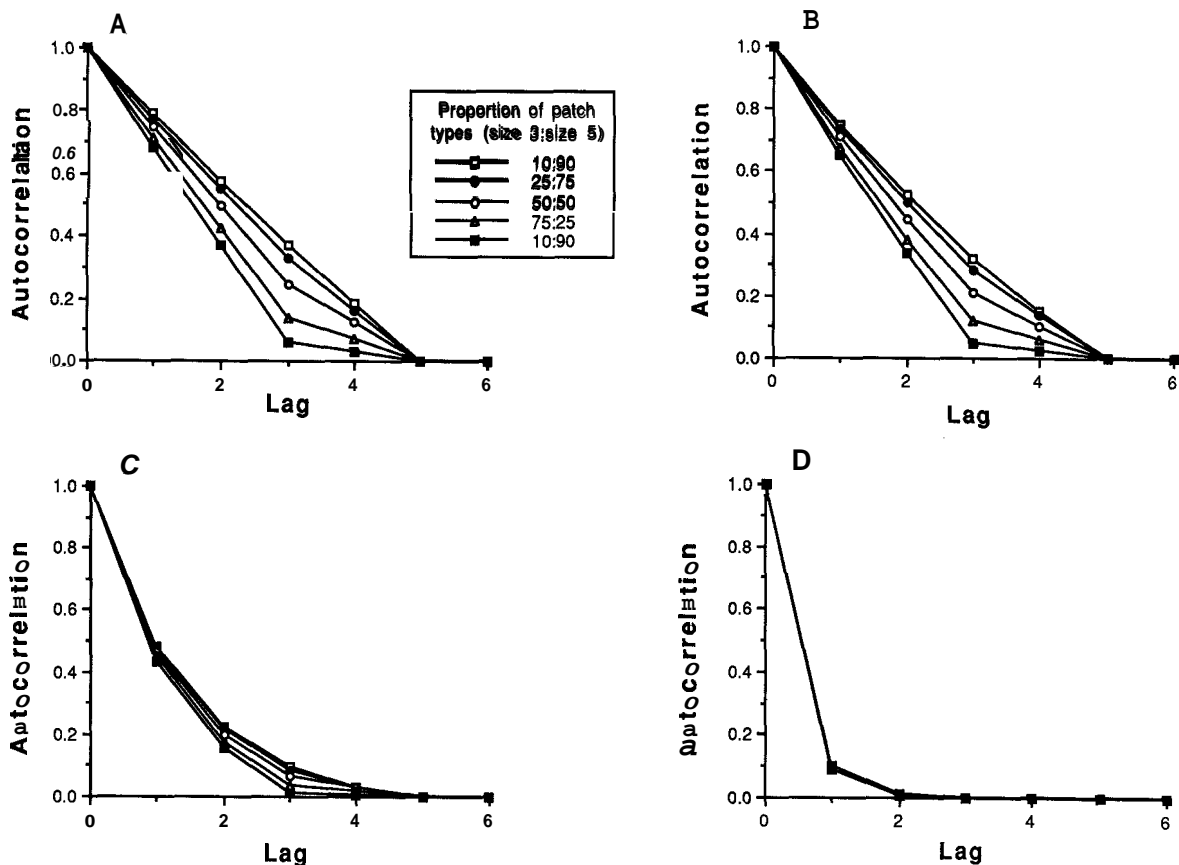


Fig. 5. Autocorrelation functions for a mixed-patch-type non-additive process with patches of size 3 and size 5 varying in relative proportion of occurrence and in probability of patch initiation. The shape of the functions was determined using Eq. 21 from the text. A) Ten disturbances initiated per 1000 sites. B) One hundred disturbances initiated per 1000 sites. C) Five hundred disturbances initiated per 1000 sites. D) Nine hundred disturbances initiated per 1000 sites.

As in the MA mixed patch-type model, the non-additive model requires two parameters for each patch type to specify the autocorrelation function and the spectrum: patch size and the probability of patch initiation.

The shape of the autocorrelation curves for different mixtures of size 3 and size 5 patches are similar to those produced by the MA mixed patch-type process if the probability of a patch being initiated is low (cf., Figs. 5a and b with Fig. 4b). However, the correspondence breaks down at higher patch densities (cf., Figs. 5c and d with Fig. 4b). This result is similar to the result found in comparing the simple one-patch-type non-additive process with the simple MA process. At low densities the non-additive process looks like the MA

process since there is little overlap among patches. At higher densities there is a high degree of overlap and information as to the underlying process is erased due to the non-additivity of patches.

Discussion

We have shown that autocorrelation analysis and spectral analysis can be used to gain insight into the size scale of critical processes contributing to pattern formation in ecological systems, at least for very simple systems. With pattern forming processes occurring at only one size scale, the power spectrum identifies the scale of the process as corresponding exactly with the local minimum in the

power spectrum that occurs at the lowest spectral frequency. This relationship always holds true if the patch forming process is strictly additive, as in the MA model, or if there is a low probability of patch overlap in a non-additive process. These cases are rather restrictive and should be viewed as a starting point for understanding the use of spectral analysis and autocorrelation analysis in interpreting more complicated, but realistic, ecological patterns.

Autocorrelation analysis may yield more immediate insight into the size scale of processes producing pattern than does spectral analysis, particularly if the pattern-forming processes are occurring at more than one size scale. For an MA process, the slope of the autocorrelation function changes at each size scale associated with the size scale of a pattern-forming process operating in the system; in fact, the amount of variance in the system attributable to patches formed at different size scales is proportional to the change in the slope of the autocorrelation function at that scale. This information can be used to determine the relative importance of patches of varying size in producing pattern. Again, the situation is more complex for systems in which the processes do not act additively. For example, in the non-additive model considered by this paper the pattern appears to be totally random if patch formation is extensive. As the probability of overlap among patches increases, information regarding the critical size scales of the process is erased, the spectrum flattens to a horizontal line, and the autocorrelation function approaches a value of zero at all non-zero lags. However, unless patch formation is extensive, a non-additive process looks very much like an MA process. Therefore, in most realistic situations some information regarding the scale of the dynamics producing pattern will be revealed through autocorrelation analysis.

Variation in the apparent size-scale of pattern forming processes, as characterized by the autocorrelation function and the spectrum, may arise through a variety of mechanisms: (i) occurrence of patch forming processes at more than one size scale; (ii) stochastic variation in the size of the patch forming process; (iii) analysis of a two dimensional

patch-forming process of fixed shape by use of a one dimensional analytical technique; (iv) negative or positive autocorrelation among patch-forming processes; and (v) non-uniform density within individual patches. Although we have only investigated item (i) explicitly in this paper, items (ii) and (iii) can be treated as special cases of item (i), given the proper perspective. In contrast, the introduction of an among-patch correlation structure or within-patch variation in density will require the development of a more sophisticated class of probability models to explore the relationships among the autocorrelation function, the power spectrum, and the processes producing pattern. It will be very important to determine which of these potential forms of variation are operating when one interprets pattern formation in natural ecosystems. This can only be done through on-site inspection and direct experimentation. However, the techniques developed here can act as a guide to suggest the appropriate range of scales to explore in characterizing the dynamics producing an observed pattern.

In studying pattern forming processes in ecological systems, two-dimensional analyses of the spectral and autocorrelation relationships might be more appropriate than the one-dimensional analyses outlined here, particularly if the processes producing pattern are spatially anisotropic. Two-dimensional analyses are easily performed using two-dimensional Fourier transforms. However, deriving analytically tractable probability models in two dimensions will not be as simple a task, making an exploration of the relationships coupling pattern to process more difficult in two dimensions than in one.

The approach taken in this paper has been to develop simple probabilistic models that produce pattern in a one-dimensional space and then explore the utility of autocorrelation analysis and spectral analysis in interpreting the nature of these processes. By extending our approach to include more complex situations, one can develop a very sophisticated set of tools (or adapt them directly from the extensive time-series analysis literature) for interpreting pattern in natural ecosystems. Indeed, a protocol for developing a deeper understanding of the processes giving rise to pattern in natural

ecosystems might include the following steps: (1) estimate the power spectrum and autocorrelation function of the pattern occurring in a natural ecosystem; (2) determine the range of size scales potentially involved in producing the pattern; (3) conduct experimental studies and field studies at the appropriate scales to understand system dynamics; (4) construct a spatially explicit model of the system, incorporating the findings obtained in step 3 (see Levin *et al.* 1989a; Moloney *et al.*, in press); (5) analyze the pattern produced by the model as in step 1 or derive the autocorrelation function analytically from the model specification; (6) compare the estimated spectrum and autocorrelation function of the natural ecosystem with those of the model system; and (7) determine if the model description is adequate, if not return to step 3. The ability to determine the relationship between pattern and system dynamics will be greatly improved as pattern formation in more sophisticated models and more complex ecosystems is analyzed through an integrated approach such as the one outlined above.

Clearly, pattern analysis alone cannot be used to determine a causal link between pattern and process, as a number of unrelated mechanisms can potentially yield the same pattern. However, pattern analysis can play a critical role in an integrated research program exploring the relationship between pattern and process.

Acknowledgments

Support for this research was provided in part by NSF grant BSR-8806202, DOE grant DE-FG02-90ER60933 and McIntire-Stennis grant NYC-183550 to SAL; by a subcontract to KAM on NSF grant BSR-8614769 to Hal Mooney; by U.S. Department of Commerce Cooperative Agreement NA88EA-H-00069 between the National Oceanic and Atmospheric Administration (NOAA) and Cornell University; by the Ecosystems Research Center of Cornell University under Cooperative Agreement CR-812685-03 from the United States Environmental Protection Agency; and by the U.S. Army Research Office through the Mathematical Sciences Institute of Cornell University. This is Ecosystems Research Center Publication ERC-232.

References

- Chatfield, C. 1984. The analysis of time series. Chapman and Hall, New York.
- Dale, M.R.T. and D.A. MacIsaac. 1989. New methods for the analysis of spatial pattern in vegetation. *J. Ecol.* 77: 78–91.
- Gardner, R.H., Milne, B.T., Turner, M. and O'Neill, R. 1987. Neutral models for the analysis of broad-scale landscape pattern. *Landsc. Ecol.* 1: 19–28.
- Greig-Smith, P. 1952. The use of random and contiguous quadrats in the study of the structure of plant communities. *Ann. Bot.* 16: 293–316.
- Haury, L., McGowan, J. and Wiebe, P. 1977. Patterns and processes in the time space scales of plankton distribution. pp. 277–328. *In* Spatial pattern in plankton communities. Edited by J.H. Steele. Plenum, New York.
- Hobbs, R.J. and Mooney, H.A. 1985. Community and population dynamics of serpentine grassland annuals in relation to gopher disturbance. *Oecologia* 67: 342–351.
- Krummel, J.R., Gardner, R.H., Sugihara, G., O'Neill, R.V. and Coleman, P.R. 1987. Landscape patterns in a disturbed environment. *Oikos* 48: 321–324.
- Levin, S.A. 1989. Challenges in the development of a theory of community and ecosystem structure and function. pp. 242–255. *In* Perspectives in Ecological Theory. Edited by J. Roughgarden, R. May and S.A. Levin. Princeton University Press, NJ, USA.
- Levin, S.A., Moloney, K.A., Buttel, L. and Castillo-Chavez, C. 1989a. Dynamical models of ecosystems and epidemics. *Fut. Gen. Comp. Syst.* 5: 265–274.
- Levin, S.A., Morin, A. and Powell, T.H. 1989b. Patterns and processes in the distribution and dynamics of Antarctic krill. pp. 281–299. *In* Scientific Committee for the Conservation of Antarctic Marine Living Resources Selected Scientific Papers Part 1, SC-CAMLR-SSP/5, CCAMLR, Hobart, Tasmania, Australia.
- Levin, S.A. and Paine, R.T. 1974. Disturbance, patch formation, and community structure. *Proceedings of the National Academy of Scientists* 71: 2744–2747.
- Levin, S.A. and Segel, L.A. 1985. Pattern generation in space and aspect. *SIAM Review* 27: 45–67.
- Milne, B.T. 1988. Measuring the fractal geometry of landscapes. *Appl. Math. Comp.* 27: 67–79.
- Moloney, K.A. 1988. Fine-scale spatial and temporal variation in the demography of a perennial bunchgrass. *Ecology* 69: 1588–1598.
- Moloney, K.A. 1990. Shifting demographic control of a perennial bunchgrass along a natural habitat gradient. *Ecology* 71: 1133–1143.
- Moloney, K.A., Levin, S.A., Chiariello, N.R. and Buttel, L. 1990. Pattern and scale in a serpentine grassland. In press.
- Ord, J.K. 1979. Time-series and spatial patterns in ecology. *In* Spatial and temporal analysis in ecology. Edited by R.M. Cormack and J.K. Ord. International Cooperative Publishing House, Fairland, Maryland, USA.
- Paine, R.T. and Levin, S.A. 1981. Intertidal landscapes: dis-

turbance and the dynamics of pattern. *Ecol. Monogr.* 51: 145–178.

Platt, T. and Denman, K.L. 1975. Spectral analysis in ecology. *Ann. Rev. Ecol. Syst.* 6: 189–210.

Powell, T.M. 1989. Physical and biological scales of variability in lakes, estuaries, and the coastal ocean. pp. 157–176. *In Perspectives in Ecological Theory*. Edited by J. Roughgarden, R. May, and S.A. Levin. Princeton University Press, NJ, USA.

Press, W.H., Flannery, B., Teukolsky, S. and Vetterling, W. 1986. Numerical recipes: the art of scientific computing. Cambridge University Press, Cambridge, England.

Reiners, W.A. and Lang, G.E. 1979. Vegetation patterns and processes in the balsam fir zone, White Mountains. *Ecology* 60: 403–417.

Ripley, B.D. 1978. Spectral analysis and the analysis of pattern in plant communities. *J. Ecol.* 66: 965–981.

Robertson, G.P. 1987. Geostatistics in ecology: interpolating with known variance. *Ecology* 68: 744–748.

Robertson, G.P., Huston, M.A., Evans, F.C. and Tiedje, J.M. 1988. Spatial variability in successional plant community: patterns of nitrogen availability. *Ecology* 69: 1517–1524.

Turner, M., Gardner, R., Dale, V. and O'Neill, R. 1989. Predicting the spread of disturbance across heterogeneous landscapes. *Oikos* 55: 121–169.

Weber, L.H., El-Sayed, S.A. and Hampton, I. 1986. The variance spectra of phytoplankton, krill and water temperature in the Antarctic Ocean south of Africa. *Deep-sea Res.* 33: 1327–1343.

Wiens, J.A. 1989. Spatial scaling in ecology. *Funct. Ecol.* 3: 385–397.

Whittaker, R.H. 1975. *Communities and Ecosystems*. MacMillan Publishing Company, New York

Appendix I

The following provides a proof of the conjecture that the first minimum of the power spectrum for the simple MA process described in the text is the first positive zero ($w > 0$) of the derivative $f'(\omega)$ (Eq. 4 of the text) and that the first minimum occurs at $\omega = 2\pi/(m+1)$, corresponding to the patch size of the underlying MA process:

Let $C_k = k \cdot (m+1-k)$. The coefficients C_k are then symmetrical about $k = (m+1)/2$; that is $C_k = C_{m+1-k}$. If m is even, then Eq. 4 of the text is equivalent to

$$\prod_{x=1}^{m/2} C_x \cdot [\sin(\omega x) + \sin(\omega(m+1-x))] = 0; \quad (1a)$$

if m is odd, since $C_{(m+1)/2} = [(m+1)/2]^2$, Eq. 4 in the text is equivalent to

$$\begin{aligned} & \{[(m+1)/2]^2 \cdot \sin(\omega[(m+1)/2]) + \sum_{x=1}^{(m-1)/2} C_x \cdot [\sin(\omega x) + \\ & \sin(\omega(m+1-x))]\} = 0. \end{aligned} \quad (2a)$$

Rearranging terms in equations (1a) and (2a), and using the fact that $2 \cdot \sin(\omega[(m+1)/2]) \cdot \cos[\omega(m+1-2x)/2] = \sin(\omega x) + \sin(\omega(m+1-x))$, we find that, for m even,

$$\sin(\omega[(m+1)/2]) \cdot \prod_{x=1}^{m/2} C_x \cdot \cos[\omega(m+1-2x)/2] = 0, \quad (1a')$$

and, for m odd,

$$\begin{aligned} & \sin(\omega[(m+1)/2]) \cdot \{[(m+1)/2]^2 + 2 \cdot \sum_{x=1}^{(m-1)/2} C_x \cdot \\ & \cos[\omega(m+1-2x)/2]\} = 0. \end{aligned} \quad (2a')$$

For future reference, we will set

$$G(\omega) = \prod_{x=1}^{m/2} C_x \cdot \cos[\omega(m+1-2x)/2]. \quad (3a)$$

The lowest, non-trivial frequency associated with the condition $\sin(\omega[(m+1)/2]) = 0$ occurs at $\omega = 2\pi / (m+1)$; this corresponds to a wavelength of $m+1$, the patch size of the MA process. The latter result proves that the patch size generating the moving average process in Eq. 3 of the text is recovered in the power spectrum as either a minimum or a maximum. It remains to be shown that it is the first minimum; to this end it suffices to show that $G(\omega)$ is positive on $(0, 2\pi / (m+1))$.

For $m/2$ even, $G(\omega)$ may be rewritten as

$$\begin{aligned} G(\omega) &= \prod_{x=1}^{m/4} [C_x \cdot \cos[\omega(m+1-2x)/2] + (m/2+1-x) \cdot \\ & x \cdot \cos[\omega(x-1/2)]] \end{aligned} \quad (4a)$$

$$= \prod_{x=1}^{m/4} H_x(\omega)$$

and, for $m/2$ odd, $G(\omega)$ may be rewritten as

$$\begin{aligned} G(\omega) &= [(m+2)/4 \cdot (3m+2)/4] \cos(\omega m/4) + \\ & \prod_{x=1}^{m/4} H_x(\omega). \end{aligned} \quad (5a)$$

The first term in (5a) is positive and decreasing over the interval in question. Furthermore, in either (4a) or (5a) we may rewrite $H_x(\omega)$ as

$$H_x(\omega) = C \cdot \cos[\omega(m+1-2x)/2] + [(m^2+2m)/4 + x(1-x)]\cos[\omega(2x-1)/2] \quad (6a)$$

Since $x \leq m/4$, the second coefficient above always exceeds the first. Furthermore, $\cos[\omega(2x-1)/2]$ is positive (because $\omega(2x-1)/2 \leq [2\pi(m/2-1)]/[2(m+1)] < \pi/2$), whereas $\cos[\omega(m+1-2x)/2]$ is negative. Therefore, to show $H_x(\omega) > 0$ on the interval, it suffices to show that $\cos[\omega(2x-1)/2] + \cos[\omega(m+1-2x)/2] > 0$. Since the first angle is in the first

quadrant and the second angle is in the second quadrant, $H_x(\omega) > 0$ if

$$\omega(2x-1)/2 < \pi - \omega(m+1-2x)/2, \quad (7a)$$

which must be the case as $\omega \leq 2\pi / (m+1)$. Since every $H_x(\omega)$ is positive, so is $G(\omega)$. Therefore, $2\pi / (m+1)$ is the first positive minimum as claimed and corresponds to the characteristic width of the patches making up the MA process.

ERRATUM

Re: Kirk A. Moloney, Antoine Morin and Simon A. Levin, Interpreting ecological patterns generated through simple stochastic processes. (Landscape Ecology volume 5 no. 3, pages 163–174, 1991)

Due to mistakes made by the publishers, there are a number of errors in the final printed version of the above-mentioned article. It concerns the following equations: 2, 3, 4, 14, 15, 16 and in the Appendix no. 1a, 1a', 3a, 4a and 5a. Underneath we give the correct equations with their numbers and the page on which they have been printed.

p. 165

$$\rho(k) = \left(\sum_{i=0}^{m-k} \beta_i \beta_{i+k} \right) / \left(\sum_{i=0}^m \beta_i^2 \right), \quad (2)$$

$$f(\omega) = (1/\pi) \cdot \left[1 + 2 \sum_{k=1}^m \rho(k) \cdot \cos(\omega k) \right], \quad (3)$$

$$f'(\omega) = (-2/(\pi(m+1))) \cdot \sum_{k=1}^m [k(m-k+1) \cdot \sin(\omega k)] = 0. \quad (4)$$

p. 168

$$X_s = \sum_{i=1}^n \sum_{j=0}^{m_i} \beta_{ij} Z_{i(s-j)}. \quad (14)$$

$$\text{Var}(X_s) = \sum_{i=1}^n \sigma_i^2 [m_i + 1]. \quad (15)$$

$$\rho(k) = \frac{\sum_{i=1}^n \sigma_i^2 [m_i + 1 - \min(k, m_i + 1)]}{\sum_{i=1}^n \sigma_i^2 [m_i + 1]} \quad (16)$$

p. 173

$$\sum_{x=1}^{m/2} C_x \cdot [\sin(\omega x) + \sin(\omega(m+1-x))] = 0; \quad (1a)$$

$$\sin(\omega[(m+1)/2]) \cdot \sum_{x=1}^{m/2} C_x \cdot \cos[\omega(m+1-2x)/2] = 0, \quad (1a')$$

$$G(\omega) = \sum_{x=1}^{m/2} C_x \cdot \cos[\omega(m+1-2x)/2]. \quad (3a)$$

$$G(\omega) = \sum_{x=1}^{m/4} [C_x \cdot \cos[\omega(m+1-2x)/2] + (m/2+1-x) \cdot x \cdot \cos[\omega(x-1/2)]] \quad (4a)$$

$$= \sum_{x=1}^{m/4} H_x(\omega)$$

$$G(\omega) = [(m+2)/4 \cdot (3m+2)/4] \cos(\omega m/4) + \sum_{x=1}^{m/4} H_x(\omega). \quad (5a)$$